Prediction of the Antagonistic Activity of Aryl Benzyl Ethers against LTD4 by Using 3D-CoMFA Model Developed with Pranlukast Analogues

Jinyoung Kim,[1] Miryung Lee,[2] Seock-yong Kang,[2] Jina Park,[1] Yoongho Lim,[1,3] Dongsoo Koh,[4] Kwan Ha Park,[5] and Youhoon Chong[1,2,*]

[1]*Division of Bioscience and Biotechnology,* [2]*Department of Molecular Biotechnology*
[3]*Bio/Molecular Informatics Center, Konkuk University, Seoul 143-701, Korea.* [*]*E-mail: chongy@konkuk.ac.kr*
[4]*Department of Applied Chemistry, Dongduk Women's University, Seoul 136-714, Korea*
[5]*Department of Marine Biomedical Sciences, Kunsan National University, Chonbuk 573-701, Korea*
Received May 16, 2006

A 3D-CoMFA model with pranlukast analogues was constructed, which could be applied to predict the antagonistic activity of aryl benzyl ether analogues against LTD4. Molecular modeling and 3D-CoMFA studies were performed on 78 pranlukast analogues and 14 aryl benzyl ethers to evaluate the antagonistic behavior of aryl benzyl ethers and provide information for further modification of this kind of compounds. The aryl benzyl ether core was found to be in excellent three dimensional match with the central planar moiety of pranlukast analogues, and the pranlukast 3D-CoMFA model could be successfully applied to predict the biological activity of aryl benzyl ether analogues.

Key Words : 3D-CoMFA, QSAR, Pranlukast, Aryl benzyl ether

Introduction

In spite of the availability of effective and relatively cheap treatments, approximately 5% of asthmatic patients remain poorly controlled. Treatment with combination inhalers, which contain a corticosteroid and long-acting adrenoceptor agoinst, is the most effective current therapy, but the poor compliance has yet to be improved with oral therapy given once daily. However, the problem of systemic side effects conferred by oral therapy necessitates the development of oral drugs to specifically treat asthma that do not have effects on normal physiological mechanisms. There is therefore a search for new therapies, particularly safe and effective oral treatments and those that are more efficacious in severe asthma.

Antileukotrienes (montelukast, pranlukast and zafirlukast, Fig. 1) were the first new class of anti-asthma treatment to be introduced in 30 years.[1] Owing to their anti-inflammatory properties, antileukotrienes have been the primary therapeutics in asthma management for several years. Although antileukotrienes have had some clinical success in asthma, they are considerably less effective and more expensive than inhaled corticosteroids.[2]

In previous studies,[3] as a continuation of our efforts to

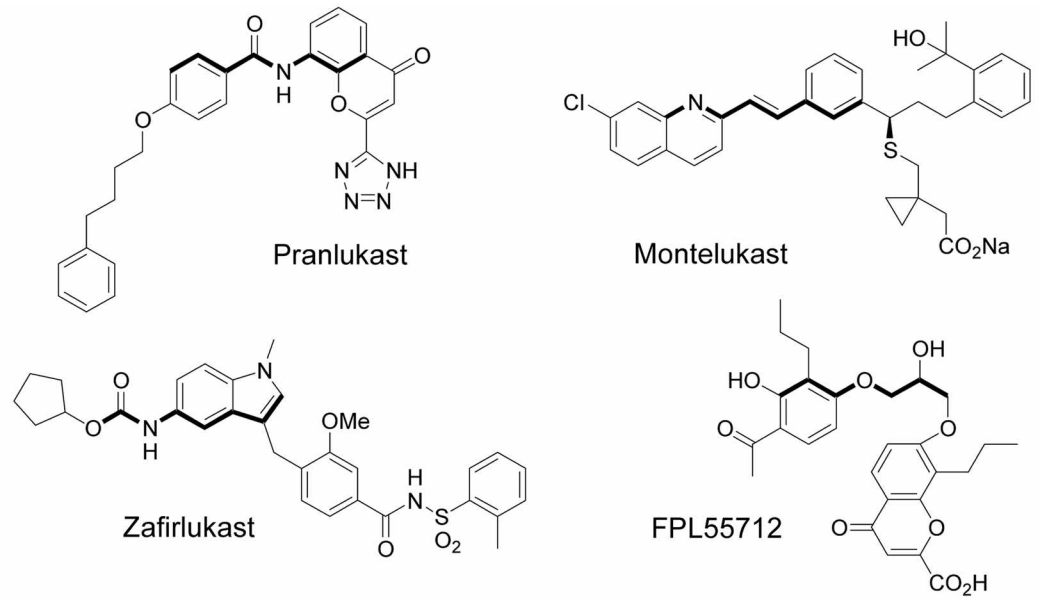

Figure 1. Structures of pranlukast, montelukast, zafirlukast, and FPL55712. The central planar triene-like moiety is shown bold.

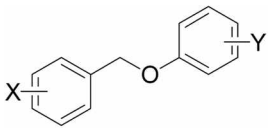

	X	Y		X	Y
1	4-OMe	4-OH	**8**	2-OMe	2-OH
2	4-OMe	3-OH	**9**	3,4-Methylenedioxy	3-OH
3	3-OMe	4-OH	**10**	3,4-Methylenedioxy	2-OH
4	3-OMe	3-OH	**11**	2,3-di-OMe	4-OH
5	3-OMe	2-OH	**12**	2,3-di-OMe	2-OH
6	2-OMe	4-OH	**13**	3,5-di-OMe	4-OH
7	2-OMe	3-OH	**14**	3,5-di-OMe	2-OH

Figure 2. Structures of aryl benzyl ethers.

develop new classes of therapeutic agents for asthma, we demonstrated that aryl benzyl ethers (Fig. 2) show interesting biological activity as leukotriene D4 (LTD4) antagonists. The promising initial assay result warrants extensive structure-activity relationship study of the aryl benzyl ethers with various substituents at the aromatic rings. However, the structure-activity relationship study has been hampered due to the large number of possible combinations of substituents on both aromatic rings. Thus, in order to make the synthetic work simple and focused, a model system which can be used to predict the effects of the aromatic substituents on the activity of aryl benzyl ethers was required.

In this study, we constructed a 3D-CoMFA model with pranlukast analogues, which could be applied to predict the antagonistic activity of aryl benzyl ether analogues against LTD4. The aim of CoMFA is to derive a correlation between the biological activity of a set of molecules and their 3D shape, electrostatic and hydrogen bonding characteristics. This correlation is derived from a series of superimposed conformations, one for each molecule in the set. These conformations are presumed to be the biologically active structures, overlaid in their common binding mode. Each conformation is taken in turn, and the molecular fields around it are calculated. Thus, a good alignment is the single most important part of doing a CoMFA analysis. The common substructure should have the same conformation in all molecules, and other parts should be superimposed as much as possible by adjusting internal torsional angles. Even though the three existing classes of antileukotriene drugs (montelukast,[4] pranlukast[5] and zafirlukast[6]) have originated from different sources, they have been eventually modified by incorporating structural components present in FPL 55712 and/or leukotriene (Fig. 1). Therefore, it is of no surprise that antileukotrienes have a planar triene-like moiety with flanking hydrophobic chain and acidic head (Fig. 1). In order to find the similar triene-like moiety in aryl benzyl ether, its lowest energy conformation was investigated by Grid search around the three rotatory bonds bridging two aromatic rings at the center of the molecule. Interestingly, the energy minimized conformation of aryl

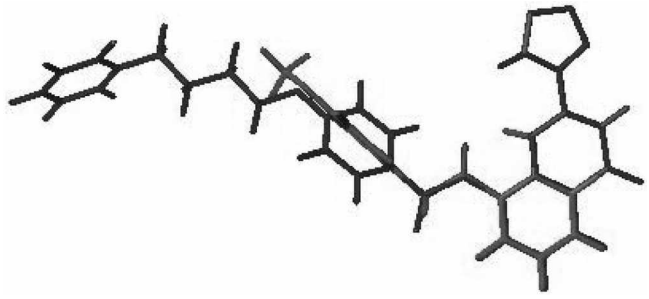

Figure 3. Superposition of pranlukast (dark) and aryl benzyl ether (**3**, light).

benzyl ether showed perfect match with the antileukotrienes around the central planar region. In particular, pranlukast and aryl benzyl ether could be superimposed atom by atom, which allowed three-dimensional structure-activity relationship study with these two series of compounds (Fig. 3).

At first, 78 pranlukast analogues were collected from the literature (**15-92**, Fig. 4).[4a] They were then randomly divided into two groups: 69 compounds as training set and the other 9 compounds as test set (Table 1). The training set was used to build 3D-CoMFA models with CoMFA (comparative molecular field analysis)[7] methods, while the test set was used to validate the 3D-CoMFA model. The model was further validated using an external test set of 14 aryl benzyl ethers (Fig. 2). Finally, the contour plots of CoMFA were analyzed to provide helpful information on how to improve the biological activity of aryl benzyl ether derivatives by structural modifications.

Materials and Methods

All calculations were carried out on a linux enterprise operating system using molecular modeling software package SYBYL v 7.2. All compounds were constructed by the Sketch module in SYBYL base, protonated and assigned with MMFF94s charges. For more flexible compounds such as aryl benzyl ethers, systematic searches were performed with an interval of 10^{o} on every rotatory bonds to ensure their lowest energy conformations. Finally, they were minimized with MMFF94s force field.

The most crucial step in performing CoMFA is to determine the bioactive conformations of the compounds so that all compounds could be aligned together. As discussed above, the central planar regions of the pranlukast analogues and aryl benzyl ethers were used as the common substructure for alignment. The most active compound among the series, pranlukast (**41**) was used as a template for structural alignment from the alignment facility in SYBYL, and 69 training set molecules, 9 test set molecules and 14 external aryl benzyl ether test set molecules were all aligned together (Fig. 5).

As usual, PLS (partial least squares) method was used to establish and validate CoMFA. The IC_{50} values were converted into pIC_{50} ($-\log IC_{50}$) values to describe the biological activities. CoMFA was set at standard values, with a sp^3

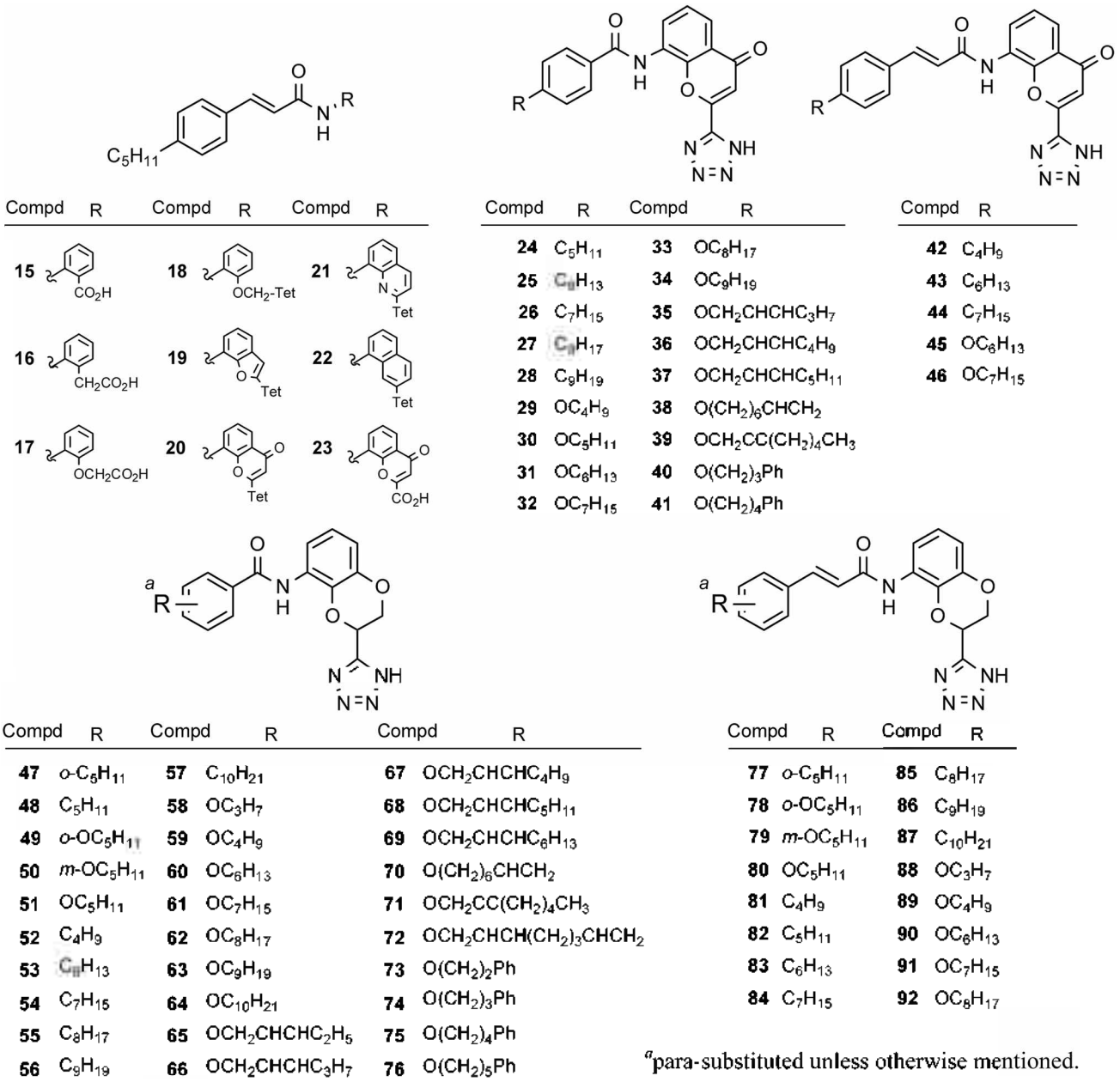

Compd	R	Compd	R	Compd	R
15	CO_2H	18	OCH_2-Tet	21	Tet
16	CH_2CO_2H	19	Tet	22	Tet
17	OCH_2CO_2H	20	Tet	23	CO_2H

Compd	R	Compd	R
24	C_5H_{11}	33	OC_8H_{17}
25	C_8H_{13}	34	OC_9H_{19}
26	C_7H_{15}	35	$OCH_2CHCHC_3H_7$
27	C_8H_{17}	36	$OCH_2CHCHC_4H_9$
28	C_9H_{19}	37	$OCH_2CHCHC_5H_{11}$
29	OC_4H_9	38	$O(CH_2)_6CHCH_2$
30	OC_5H_{11}	39	$OCH_2CC(CH_2)_4CH_3$
31	OC_6H_{13}	40	$O(CH_2)_3Ph$
32	OC_7H_{15}	41	$O(CH_2)_4Ph$

Compd	R
42	C_4H_9
43	C_6H_{13}
44	C_7H_{15}
45	OC_6H_{13}
46	OC_7H_{15}

Compd	R	Compd	R	Compd	R
47	*o*-C_5H_{11}	57	$C_{10}H_{21}$	67	$OCH_2CHCHC_4H_9$
48	C_5H_{11}	58	OC_3H_7	68	$OCH_2CHCHC_5H_{11}$
49	*o*-OC_5H_{11}	59	OC_4H_9	69	$OCH_2CHCHC_6H_{13}$
50	*m*-OC_5H_{11}	60	OC_6H_{13}	70	$O(CH_2)_6CHCH_2$
51	OC_5H_{11}	61	OC_7H_{15}	71	$OCH_2CC(CH_2)_4CH_3$
52	C_4H_9	62	OC_8H_{17}	72	$OCH_2CHCH(CH_2)_3CHCH_2$
53	C_8H_{13}	63	OC_9H_{19}	73	$O(CH_2)_2Ph$
54	C_7H_{15}	64	$OC_{10}H_{21}$	74	$O(CH_2)_3Ph$
55	C_8H_{17}	65	$OCH_2CHCHC_2H_5$	75	$O(CH_2)_4Ph$
56	C_9H_{19}	66	$OCH_2CHCHC_3H_7$	76	$O(CH_2)_5Ph$

Compd	R	Compd	R
77	*o*-C_5H_{11}	85	C_8H_{17}
78	*o*-OC_5H_{11}	86	C_9H_{19}
79	*m*-OC_5H_{11}	87	$C_{10}H_{21}$
80	OC_5H_{11}	88	OC_3H_7
81	C_4H_9	89	OC_4H_9
82	C_5H_{11}	90	OC_6H_{13}
83	C_6H_{13}	91	OC_7H_{15}
84	C_7H_{15}	92	OC_8H_{17}

[a]para-substituted unless otherwise mentioned.

Figure 4. Structures of pranlukast analogues. [a]para-substituted unless otherwise mentioned.

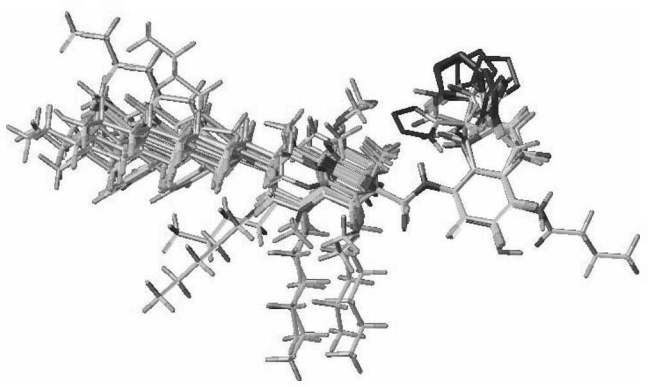

Figure 5. Superposition of 69 training set molecules, 9 test set molecules, and 14 external test set molecules (aryl benzyl ethers).

carbon atom with one positive charge used to probe steric and electrostatic fields. The standard cutoff value was set to 30 kcal/mol. LOO (leave-one-out) cross-validation method was used to evaluate the initial model. The cross-validated coefficient q^2 was calculated using the following equation:

$$q^2 = 1.0 - \frac{\sum_{\gamma} (\gamma_{\text{pred}} - \gamma_{\text{actual}})^2}{\sum_{\gamma} (\gamma_{\text{actual}} - \gamma_{\text{mean}})^2}$$

where γ_{pred}, γ_{actual}, and γ_{mean} are predicted, actual, and mean values of the target property (pIC_{50}), respectively, and PRESS = $\Sigma_{\gamma}(\gamma_{\text{pred}} - \gamma_{\text{actual}})^2$ is the sum of predictive sum of squares. The optimum number of components was then

Table 1. CoMFA analysis on pranlukast analogues

PRESS	q^2	N	r^2	SEE	F	SEEbs	q^2_{bs}	Pred. r^2
3.91	0.845	5	0.971	0.249	258.8	0.214	0.981	0.938[a] 0.599[b]

q^2-leave one out (LOO) cross-validated correlation coefficient, *N*-optimum number of components, r^2-noncross-validated correlation coefficient, SEE-standard error of estimate, F-F-test value, SEEbs-standard error of estimate by boot strapping analysis, q^2_{bs}-mean r^2 by boot strapping analysis (in 10 runs), Pred. r^2-CoMFA predictive q^2 values on the test set: [a]test set composed of 9 pranlukast analogues, [b]external test set composed of 14 aryl benzyl ethers.

given, and CoMFA model was finally derived corresponding to the optimum number. The parameters of confidence intervals were further estimated by bootstrap in 10 runs. The column filtering box was kept unchecked during all operations (Table 1).

In addition to LOO method to validate the CoMFA model, two test sets made up of 9 and 14 molecules, respectively, was used for model validation. Similar to cross-validated q^2 values of LOO method, the predictive performance of models on the test set was estimated by predictive r^2 value (Table 1).

Results and Discussion

The best prediction was obtained with CoMFA standard model (*PRESS* = 3.91, $q^2 = 0.845$, $N = 5$), and its predictive performance on the test was $r^2 = 0.971$, which indicated that the built 3D-CoMFA model was reliable and able to predict biological activity of new derivatives accurately (Table 1). The relative contribution of steric and electrostatic field to the overall CoMFA field is 0.642 and 0.358, respectively, which indicates dominant contribution by the steric factor. Also, the predictive r^2 values for both test sets were greater than 0.5, which indicates significant predictive power of the model.

The conventional fit values on training set and prediction values on the test set made by the CoMFA model is shown in Table 2. The relationship curve between observed values versus conventional fit values (prediction values) on the training set and two test sets are also displayed in Fig. 6.

CoMFA result is visualized by 'stDev*Coeff' contours, which shows that there is a large green contour around the phenyl ring at the end of the hydrophobic alkyl chain (Fig. 7a). Interestingly, the alkyl chain has a discrete length for optimum activity, and thus, even a slightly longer chain results in unfavorable steric interaction (yellow contour next to green one). Also, the small yellow contours around the alkyl chain indicate that branched alkyl chains would have unfavorable steric interaction. On the other hand, around the tetrazole moiety electrostatic interaction is favored (blue contour, Fig. 7b). The fused rings are sandwiched between two red contours, which show that the fused rings should remain planar between these two contours. The small blue contour around the aromatic alkyl substituent indicates that substitution of the alkyl chain with charged heteroatoms

Table 2. Actual versus predicted activity of CoMFA (standard) model on the training set and test set

Compds	pIC_{50}[a] (act)[b]	pIC_{50} (pred)[c]	Res	Compds	pIC_{50} (act)[b]	pIC_{50} (pred)[c]	Res
(a) Training set							
15	4.85	4.97	−0.12	**57**	6.30	6.32	−0.02
16	4.70	4.80	−0.10	**58**	5.66	6.31	−0.65
18	5.52	5.40	0.13	**59**	6.66	6.51	0.14
19	5.51	5.53	−0.02	**60**	7.89	7.97	−0.08
21	6.00	5.89	0.11	**62**	7.85	7.89	−0.03
22	6.52	6.56	−0.03	**63**	7.70	7.11	0.59
23	6.62	6.52	0.10	**64**	6.52	6.51	0.01
24	6.74	7.03	−0.28	**65**	6.82	7.01	−0.18
25	7.82	7.43	0.40	**66**	8.37	8.12	0.25
26	8.38	8.54	−0.17	**68**	8.70	8.72	−0.02
27	8.26	8.55	−0.29	**69**	8.28	8.18	0.10
29	8.30	7.56	0.75	**70**	8.89	8.59	0.30
30	7.28	7.80	−0.52	**71**	9.17	9.20	−0.03
31	9.07	8.89	0.17	**72**	8.96	9.32	−0.36
32	9.30	9.43	−0.13	**73**	7.21	7.18	0.03
33	8.26	8.72	−0.46	**74**	7.70	7.76	−0.06
34	8.13	8.16	−0.02	**75**	9.43	9.37	0.06
35	8.82	9.03	−0.21	**76**	7.96	8.11	−0.15
37	10.22	9.56	0.66	**77**	5.67	5.48	0.19
38	9.96	9.78	0.18	**78**	5.64	5.49	0.15
39	9.85	9.98	−0.13	**79**	6.82	6.99	−0.17
40	9.02	8.98	0.04	**80**	6.92	7.19	−0.26
41	10.36	10.41	−0.05	**81**	6.31	6.16	0.15
42	7.47	7.35	0.12	**82**	6.66	6.62	0.03
44	7.00	7.12	−0.11	**83**	6.85	6.81	0.04
45	7.74	7.62	0.12	**84**	6.46	6.52	−0.06
46	6.85	6.94	−0.08	**85**	6.24	6.12	0.12
47	4.40	4.54	−0.15	**86**	5.49	5.68	−0.18
49	5.03	4.98	0.04	**87**	5.96	5.65	0.31
50	5.30	5.28	0.02	**88**	6.18	6.18	0.00
52	5.82	5.85	−0.03	**89**	6.92	6.76	0.16
53	6.68	6.75	−0.07	**90**	7.68	7.38	0.30
54	7.15	7.00	0.16	**91**	7.06	7.16	−0.11
55	7.00	6.90	0.10	**92**	6.67	6.94	−0.27
56	6.80	6.74	0.06				
(b) Test set[d]							
17	5.05	4.79	0.25	**48**	5.59	6.33	−0.74
20	7.52	7.39	0.13	**51**	7.00	6.95	0.05
28	8.15	8.03	0.12	**61**	8.05	8.35	−0.31
36	10.51	9.75	0.76	**67**	9.33	9.03	0.30
43	7.49	7.63	−0.13				
(c) External test set[e]							
1	5.11	4.38	0.73	**8**	4.48	4.07	0.41
2	4.74	4.29	0.45	**9**	4.18	4.45	−0.27
3	5.42	4.36	1.06	**10**	4.82	4.88	−0.06
4	4.65	4.62	0.03	**11**	4.33	4.60	−0.27
5	4.39	4.80	−0.41	**12**	4.32	4.17	0.15
6	4.16	3.74	0.42	**13**	4.59	4.43	0.16
7	4.45	4.47	−0.02	**14**	4.68	4.77	−0.09

[a]$pIC_{50} = -\log IC_{50}$; [b]actual activity; [c]predicted activity; [d]test set of 9 pranlukast analogues; [e]test set of 14 aryl benzyl ethers

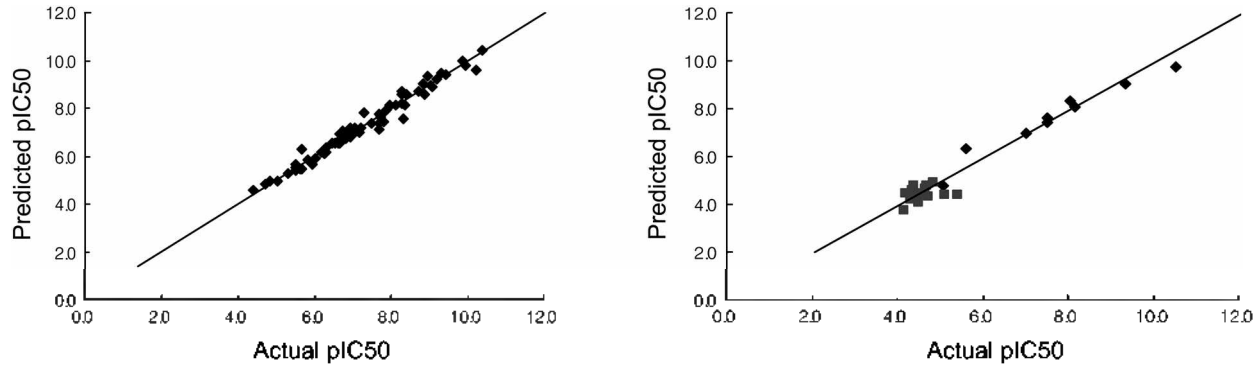

Figure 6. Plot of observed pIC_{50} versus conventional fit predictions (predicted activity) of training set (a) and test set (b). Gray dot show conventional fit (prediction) of aryl benzyl ethers.

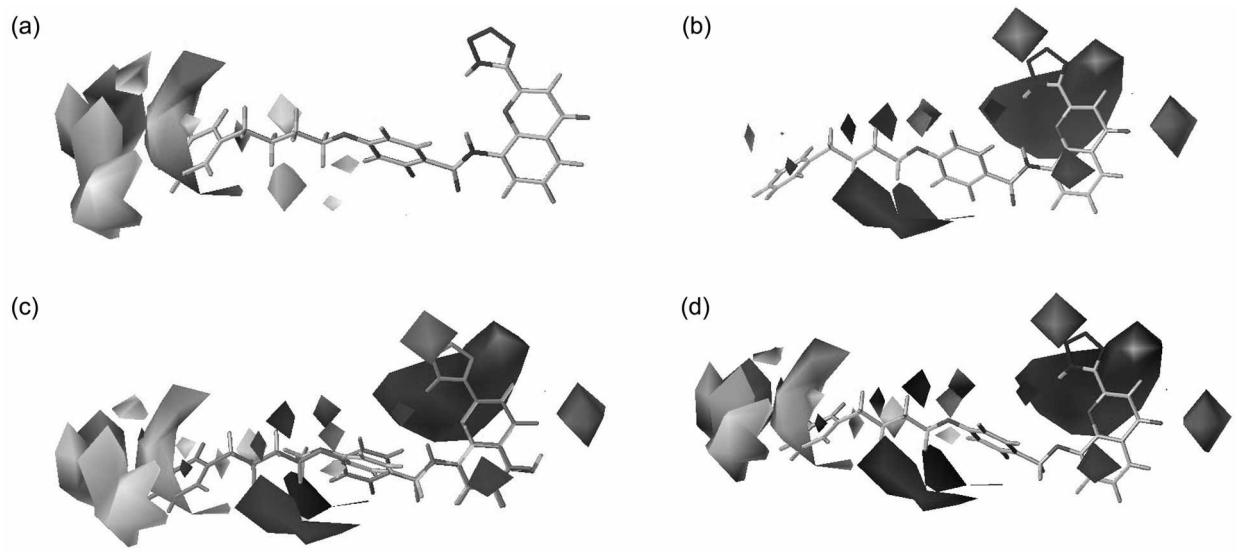

Figure 7. CoMFA (standard model) Contour plots: pranlukast (**41**) is depicted as a reference molecule: (a) light contours predict bulky group enhance activity, whereas dark contours predict less bulky group is favored for activity; (b) light contours predict negative charge enhance activity, whereas dark contours predict positive charge enhance activity; (c) pranlukast (**41**) and **1** are shown together inside the combined map of steric and electrostatic contours; (d) aryl benzyl ether with pranlukast-like substitution is located inside the contour map.

such as oxygen, or nitrogen would favor electrostatic interaction. Aryl benzyl ether **1** is located inside the combined map of steric and electrostatic contours with pranlukast (Fig. 7c), which provides insights into the structural modification of the aryl benzyl ether to improve its activity. As an example, a compound with simple introduction of the aromatic substituents of pranlukast (**41**) into the aryl benzyl ether core (Fig. 7d) snuggly fits into the contour map, and the QSAR program expects this compound to be even more active than pranlukast (predicted pIC_{50} for this compound is 10.83).

Based on this information, various alkyl chains with optimum chain length and fused aromatic rings with polar substituents are being designed and installed onto the aryl benzyl ether core structure. The extensive structure-activity relationship study of aryl benzyl ethers as a novel class of antileukotriene would be reported in due course.

Conclusions

In summary, even though leukotriene modifiers have been used for asthma treatment for several years, problems associated with the current therapy such as the lack of clinical efficacy for severe asthma and the lack of specific LTB4 antagonists[8] have continuously prompted the discovery of novel leukotriene modifiers. Due to the promising biological activity as leukotriene D4 (LTD4) antagonists,[5-8] extensive structure-activity relationship study of the aryl benzyl ethers with various substituents at the aromatic rings are underway. In this study, in order to design an efficient structure-activity relationship study of aryl benzyl ethers, a 3D-CoMFA model was constructed by using the pranlukast analogues. The aryl benzyl ether core was found to be in excellent three dimensional match with the central planar moiety of pranlukast analogues, and the pranlukast 3D-

CoMFA model could be successfully applied to predict the biological activity of aryl benzyl ether analogues. The 3D-CoMFA study also shows that hydrophobic alkyl chain with optimum length substituted at the benzylic aromatic ring as well as highly charged fused aromatic moiety at the other side of aryl benzyl ether core would greatly enhance the biological activity of aryl benzyl ether analogues.

Acknowledgments. This work was supported by a grant Biogreen 21 (Korea Ministry of Agriculture and Forestry) and the second Brain Korea 21 (Korea Ministry of Education). Jinyoung Kim is supported by the second Brain Korea 21.

References

1. Drazen, J. M.; Israel, E.; O'Byrne, P. M. *N. Engl. J. Med.* **1999**, *340*, 197.
2. Barnes, P. J. *Curr. Opin. Pharmacol.* **2003**, *3*, 257.
3. (a) Koh, D.; Park, K. H.; Lee, H.; Jung, J.; Cho, S. K.; Lim, Y. *Agric. Chem. Biotechnol.* **2000**, *43*, 277. (b) Koh, D.; Park, K. H.; Lee, H.; Jung, J.; Kim, K.; Cho, S. K.; Lim, Y. *Agric. Chem. Biotechnol.* **2000**, *43*, 281. (c) Koh, D.; Park, K. H.; Lim, Y. *Agric. Chem. Biotechnol.* **2001**, *44*, 35. (d) Koh, D.; Park, K. H.; Lee, H.; Jung, J.; Lim, Y. *Agric. Chem. Biotechnol.* **2001**, *44*, 32.
4. (a) Nakai, H.; Konno, M.; Kosuge, S.; Sakuyama, S.; Toda, M.; Arai, Y.; Obata, T.; Katusbe, N.; Miyamoto, T.; Okegawa, T.; Kawasaki, A. *J. Med. Chem.* **1988**, *31*, 84. (b) Taniguchi, Y.; Tamura, G.; Honma, M.; Aizawa, T.; Maruyama, N.; Shirato, K.; Takishima, T. J. *Allergy Clin. Immunol.* **1993**, *92*, 507.
5. (a) Bernstein, P. R.; Bird, T. G.; Brewster, A. G. In *Burger's Medicinal Chemistry and Drug Discovery*; Wolff, M. E., Ed.; Wiley: New York, 1997; Vol. 5, pp 405-493. (b) Jones, T. R.; Labelle, M.; Belley, M.; Champion, E.; Charette, L.; Evans, J.; Ford-Hutchinson, A. W.; Gauthier, J.-Y.; Lord, A.; Masson, P.; McAuliffe, M.; McFarlane, C. S.; Metters, K. M.; Pickett, C.; Piechuta, H.; Rochette, C.; Rodger, I. W.; Sawyer, N.; Young, R. N.; Zamboni, R.; Abraham, W. M. *Can. J. Physiol. Pharmacol.* **1995**, *73*, 191.
6. (a) Brown, F. J.; Yee, Y. K.; Cronk, L. A.; Hebbel, K. C.; Krell, R. D.; Snyder, D. W. *J. Med. Chem.* **1990**, *33*, 1771. (b) Yee, Y. K.; Brown, F. J.; Hebbel, K. C.; Cronk, L. A.; Snyder, D. W.; Krell, R. D. *Ann. N. Y. Acad. Sci.* **1988**, *524*, 458.
7. (a) Cramer, R. D., III; Patterson, D. E.; Bunce, J. D. *J. Am. Chem. Soc.* **1988**, *110*, 5959. (b) Lee, D. Y.; Hyun, K. H.; Park, H. Y.; Lee, K. A.; Lee, B.-S.; Kim, C. K. *Bull. Korean Chem. Soc.* **2006**, *27*, 273. (c) Myung, P.-K.; Park, K.-Y.; Sung, N.-D. *Bull. Korean Chem. Soc.* **2005**, *26*, 1941.
8. Ando, K.; Tsuji, E.; Ando, Y.; Kunitomo, J.-I.; Kobayashi, R.; Yokomizo, T.; Shimizu, T.; Yamashita, M.; Ohta, S.; Nabe, T.; Kohno, S.; Ohishi, Y. *Org. Biomol. Chem.* **2005**, *3*, 2129.